

# Calibrating systematic errors in the distance determination with the luminosity-distance space large scale structure of dark sirens and its potential applications

Pengjie Zhang<sup>1,2,3</sup>, Hai Yu<sup>1,2</sup>

<sup>1</sup>*Department of Astronomy, School of Physics and Astronomy, Shanghai Jiao Tong University, Shanghai, 200240, China*

<sup>2</sup>*Key Laboratory for Particle Astrophysics and Cosmology (MOE)/Shanghai Key Laboratory for Particle Physics and Cosmology, China*

<sup>3</sup>*Tsung-Dao Lee Institute, Shanghai Jiao Tong University, Shanghai 200240, China*

*Email to: zhangpj@sjtu.edu.cn; yu\_hai@sjtu.edu.cn*

11 August 2021

## ABSTRACT

The cosmological luminosity-distance can be measured from gravitational wave (GW) standard sirens, free of astronomical distance ladders and the associated systematics. However, it may still contain systematics arising from various astrophysical, cosmological and experimental sources. With the large amount of dark standard sirens of upcoming third generation GW experiments, such potential systematic bias can be diagnosed and corrected by statistical tools of the large scale structure of the universe. We estimate that, by cross-correlating the dark siren luminosity-distance space distribution and galaxy redshift space distribution, multiplicative error  $m$  in the luminosity distance measurement can be constrained with  $1\sigma$  uncertainty  $\sigma_m \sim 0.1$ . This is already able to distinguish some binary black hole origin scenarios unambiguously. Significantly better constraints and therefore more applications may be achieved by more advanced GW experiments.

**Key words:** Cosmology: large-scale structure of Universe, gravitational waves

## 1 INTRODUCTION

About 50 gravitational wave (GW) events of binary compact star coalescence have been detected by advanced LIGO and advanced Virgo collaboration (LVC) (Abbott et al. 2016, 2017b,c,d, 2019a, 2020b,c; The LIGO Scientific Collaboration et al. 2020a; Abbott et al. 2020a; The LIGO Scientific Collaboration et al. 2020b). The total number of detections will be dramatically increased by three orders of magnitude by the third generation GW experiments such as the proposed Einstein Telescope (ET<sup>1</sup>) and Cosmic Explorer (CE, Dwyer et al. (2015); Abbott et al. (2017a); Reitze et al. (2019)). These experiments will be able to detect binary black holes (BBHs) within our horizon (Dwyer et al. 2015). Given the estimated BBH merger rate  $R = 53.2_{-28.8}^{+58.5} \text{ Gpc}^{-3} \text{ yr}^{-1}$  (90% credibility, Abbott et al. (2019b)),  $\sim 10^5$  BBH detections per year are achievable. The angular localization accuracy will improve to  $\lesssim 1 \text{ deg}^2$ , and the measurement accuracy of luminosity-distance through the standard siren method (Schutz 1986; Abbott et al. 2017e) will reach  $\sigma_D/D \lesssim 0.1$  (Zhao & Wen 2018). The detection of higher spherical harmonics beyond the quadrupole mode (GW190814, Abbott et al. (2020c) & GW190412, The LIGO Scientific Collaboration et al. (2020a)) and the

analysis using the full waveforms instead of the restricted waveforms (Arun et al. 2007; Van Den Broeck & Sengupta 2007; Ajith & Bose 2009; Roy et al. 2019) will lead to further significant improvement in the angular resolution and distance determination.

Binary neutron star (BNS) GW events have weaker amplitude, so the redshift coverage, angular resolution and distance determination accuracy by ET and CE will be significantly worse than that of BBH GW events (Zhao & Wen 2018; Reitze et al. 2019). Nevertheless, more ambitious GW experiments such as Big Bang Observer (BBO, Cutler & Harms (2006)) are capable of achieving 1% distance measurement and arcminute angular localization. Since BNS event rate is an order of magnitude higher (Abbott et al. 2017d, 2019a, 2020b), eventually we would expect  $\sim 10^6$  GW events (mostly BNS events) per year of known 3D positions all over the observable universe.

These upcoming 3D mappings of the universe through GW events will enable the measurement and application of a new type of large scale structure (LSS) of the universe, namely the luminosity-distance space LSS (Zhang 2018a,b; Namikawa 2020; Libanore et al. 2020). Most of these GW events will not have electromagnetic (EM) counterparts or host galaxies identified, so the usual standard siren cosmology techniques (Schutz 1986; Holz & Hughes 2005; Cutler & Holz 2009; Abbott et al. 2017e; Soares-Santos et al. 2019; The LIGO Scientific Collaboration et al. 2019) are not

<sup>1</sup> <https://www.et-gw.eu/>

applicable. Nevertheless, these dark standard sirens construct an excellent data set of LSS. Due to the fact that gravitational waves are transparent while EM waves are not, the observed GW event spatial distribution is immune to galactic and extragalactic contaminations. Its spatial selection function is expected to be more homogeneous and well understood. Together with the potentially full coverage of cosmic volume within the horizon, the luminosity-distance space LSS is promising to provide clean information on all linear LSS modes of our universe. Furthermore, this LSS is spatially correlated with the usual LSS in redshift space and various 2D projections (e.g. weak lensing), making them highly complementary (Zhang 2018a,b; Namikawa et al. 2016; Oguri 2016; Nair et al. 2018; Mukherjee & Wandelt 2018; Soares-Santos et al. 2019; The LIGO Scientific Collaboration et al. 2019).

The dark siren based LSS does not require EM identification of EM counterparts or host galaxies. However, all promising applications of the dark siren based LSS are built on unbiased measurement of the luminosity-distance  $D_L^{\text{obs}}$ , with respect to the cosmological luminosity-distance  $D_L^{\text{cos}}$ . Various experimental, astrophysical, and cosmological issues may cause systematic bias in the distance measurement, analogous to redshift measurement in EM observations. (1) The most obvious one is calibration error in the GW strain amplitude (e.g. Sun et al. (2020)). Although it is expected to be small (several percent for current experiments), independent verification is useful. Calibration errors also affect the phase and therefore the inferred distance. (2) One example of cosmological issues is modification to general relativity, which may affect the GW propagation and/or the GW generation (e.g. Deffayet & Menou (2007); Belgacem et al. (2018); Ezquiaga & Zumalacárregui (2018)). If graviton has mass or if it can propagate in extra dimensions, the resulting  $D_L^{\text{obs}}$  will be larger than the corresponding luminosity-distance of EM counterpart, which equals to the luminosity-distance ( $D^{\text{cos}}$ ) of the FRW universe. (3) One example of astrophysical issues is related to the environment of GW events. This is motivated by the challenge in explaining the origin of high mass BBH ( $\gtrsim 20M_\odot$ ) by stellar evolution models. Chen et al. (2019) argued that the observed ‘‘high mass’’ BBHs may preferentially reside within  $\lesssim 10$  Schwarzschild radius of the supermassive black hole of host galaxies. These BBH events then suffer an extra gravitational redshift  $z_{\text{gra}}$  and an extra Doppler redshift  $z_{\text{Dop}}$ . The inferred black hole masses will be overestimated by  $(1 + z_{\text{gra}})(1 + z_{\text{Dop}})$ . In this scenario, the inferred luminosity-distance is overestimated by the same factor,  $D_L^{\text{obs}} = D_L^{\text{cos}}(1 + z_{\text{gra}})(1 + z_{\text{Dop}})$ . This effect can lead to a factor of  $\sim 2$  bias in  $D_L$ . Other BBH environment effects may also exist. Gas around the BBH orbit affects the orbital motion and therefore affects the GW waveform (Chen & Shen 2019). Although this effect is likely negligible for high frequency observations such as LIGO, ET and CE, this demonstrates the need to comprehensive investigation of BBH environment and its impact on the  $D_L$  determination.

Given the possible existence of significant systematic error in  $D_L$ , standard siren cosmology will be significantly impacted. It is the purpose of this paper to provide a model-independent method of diagnosing and correcting such systematics. Significant systematic error in  $D_L$  would cause abnormal behavior in the angular correlation of GW dark sirens and galaxy distributions. Similar behavior is well known

in the context of LSS. One early application is the SZ tomography (Zhang & Pen 2001; Shao et al. 2011), where cross-correlating wit galaxies help recover the redshift information of the thermal Sunyaev Zel’dovich (SZ) effect. It is also widely used in the cross calibration (Newman 2008) and the self-calibration of galaxy photometric redshift errors (Schneider et al. 2006; Zhang et al. 2010, 2017). Similar techniques have been designed to identification of dark siren redshifts (Namikawa et al. 2016; Oguri 2016; Nair et al. 2018; Mukherjee & Wandelt 2018; Zhang 2018b). The question is to convert the directly measured cross correlation into unbiased constraint on systematic error in  $D_L$ . We find that this problem is essentially identical to identify the true redshift distribution of GW dark sirens. For the later purpose, we have proposed the  $E_z$  estimator (Zhang 2018b). It is essentially the same estimator that one of the authors proposed in the context of SZ tomography (Zhang & Pen 2001). Zhang (2018b) proved that, it is unbiased in recovering the true redshift distribution, insensitive to model assumptions on dark siren and galaxy distribution. The same  $E_z$  estimator, when applying to the current problem, will not only diagnose the existence of systematic bias in  $D_L$ , but also constrain it unbiasedly.

This paper is organized as follows. In §2, we briefly describe the  $E_z$  estimator in the context of calibrating systematic error in  $D_L^{\text{obs}}$ . In §3 we estimate its constraining power. In term of the multiplicative error  $m$ , we find that ET and CE, together with pre-existing galaxy surveys, will be able to constrain with  $\sigma_m \sim 0.1$ . We discuss and summarize in §4.

## 2 CROSS-CALIBRATION WITH THE $E_z$ ESTIMATOR

Any error leading to  $\langle D_L^{\text{obs}} - D_L^{\text{cos}} \rangle \neq 0$  belongs to systematic error. Following the common parametrization in cosmic shear measurements (Heymans et al. 2006; Massey et al. 2007), we can classify them into multiplicative errors and additive errors,

$$D_L^{\text{obs}} = D_L^{\text{cos}}(1 + m) + \epsilon. \quad (1)$$

$\epsilon$  is the additive error. When  $\langle \epsilon \rangle \neq 0$  or when  $\epsilon$  has spatial correlation (analogous to the galaxy intrinsic alignment in cosmic shear), it is a systematic error. Otherwise it will be the statistical error in the distance determination. For the current paper, we will only consider the later case, as would be caused by instrumental noise of GW experiments. Namely we consider  $\epsilon$  as a random variable with zero mean and pdf  $p(\epsilon)$ . For brevity, we assume  $p(\epsilon)$  to be Gaussian, with  $\sigma_\epsilon = \sigma_{D_L^{\text{obs}}}$ .  $m$  is the multiplicative error in the luminosity-distance determination, and  $\langle m \rangle \neq 0$ . As discussed in the previous section, it can have various origins. For the astrophysical origin proposed by Chen et al. (2019),  $1 + m = (1 + z_{\text{gra}})(1 + z_{\text{Dop}})$ . Chen et al. (2019) argued that for BBHs with mass  $\gtrsim 20M_\odot$ ,  $m \sim 1$ . But BBHs with lower mass may reside in different environments and are free of this bias. Therefore later we will consider two fiducial cases of  $m = 0$  and  $m = 1$ .

With the presence of  $m \neq 0$ , the true redshift distribution

of dark sirens within a distance bin ( $D_1 < D_L^{\text{obs}} < D_2$ ) is

$$\begin{aligned} \bar{n}_{\text{GW}}^{\text{cos}}(z) &= \int_{D_1}^{D_2} dD_L^{\text{obs}} \int_0^\infty dD_L^{\text{cos}} \delta_D(z - z(D_L^{\text{cos}})) \\ &\times p(D_L^{\text{cos}} | D_L^{\text{obs}}) n_{\text{GW}}^{\text{obs}}(D_L^{\text{obs}}). \end{aligned} \quad (2)$$

Here  $n_{\text{GW}}^{\text{obs}}(D_L^{\text{obs}})$  is the number of dark sirens per unit  $D_L^{\text{obs}}$  interval.  $p(D_L^{\text{cos}} | D_L^{\text{obs}})$  is the PDF of  $D_L^{\text{cos}}$  given  $D_L^{\text{obs}}$ . It is determined by the statistical error ( $\epsilon$ ) probability distribution  $p(\epsilon)$  and  $m$ , where  $\epsilon = D_L^{\text{obs}} - D_L^{\text{cos}}(1 + m)$ . Fluctuations in the dark siren surface density is then

$$\delta_{\text{GW}}^\Sigma(\hat{\theta}) = \bar{\Sigma}_{\text{GW}}^{-1} \left[ \int_0^\infty \delta_{\text{GW}}(z, \hat{\theta}) \bar{n}_{\text{GW}}^{\text{cos}}(z) dz \right]. \quad (3)$$

Here the mean surface number density

$$\bar{\Sigma}_{\text{GW}} = \int_{D_1}^{D_2} \bar{n}_{\text{GW}}^{\text{obs}}(D_L^{\text{obs}}) dD_L^{\text{obs}} = \int_0^\infty \bar{n}_{\text{GW}}^{\text{cos}}(z) dz. \quad (4)$$

$\delta_{\text{GW}}(z, \hat{\theta})$  is the number overdensity of dark sirens at cosmological redshift  $z$  and angular direction  $\hat{\theta}$ .

These dark sirens have angular cross-correlation with galaxies. We have the freedom to weigh the galaxy number distribution  $n_g(z)$  with an arbitrary weighting function  $W_g(z)$ . For the weighted galaxy distribution,

$$\delta_g^\Sigma(\hat{\theta}) = \bar{\Sigma}_g^{-1} \left[ \int_0^\infty \delta_g(z, \hat{\theta}) \bar{n}_g(z) W_g(z) dz \right]. \quad (5)$$

Here the mean galaxy surface number density  $\bar{\Sigma}_{g,j} = \int_0^\infty \bar{n}_g(z) W_g(z) dz$ . The GW-galaxy cross and galaxy auto angular power spectra at multipole  $\ell$  are

$$C^{\text{GW-g}}(\ell) = \frac{\int P_{\text{GW-g}}(k, z) \bar{n}_{\text{GW}}^{\text{cos}} \bar{n}_g W_g \chi^{-2} \frac{dz}{d\chi} dz}{\bar{\Sigma}_{\text{GW}} \bar{\Sigma}_g}, \quad (6)$$

$$C^g(\ell) = \frac{\int P_g(k, z) (\bar{n}_g W_g)^2 \chi^{-2} \frac{dz}{d\chi} dz}{\bar{\Sigma}_g^2}. \quad (7)$$

Here  $\chi$  is the comoving radial distance.  $P_g(k, z)$  and  $P_{\text{GW-g}}(k, z)$  are the 3D galaxy and galaxy-GW host galaxy power spectrum respectively, with  $k = \ell/\chi(z)$  in the above integrals. The above expressions adopt a flat universe cosmology. But the methodology holds for curved universe as well.

The true redshift distribution (or  $m$ ) of GW dark standard sirens can be obtained by maximizing the  $E_z$  estimator (Zhang 2018b),

$$E_z(\ell | W_g) = \frac{C_{\text{GW-g}}(\ell | W_g)}{\sqrt{C_g(\ell | W_g)}}. \quad (8)$$

Here we highlight the dependence of  $E_z$ ,  $C_{\text{GW-g}}$  and  $C_g$  on the weighting function  $W_g$ . By varying  $W_g$  to find the maximum of  $E_z$ , unbiased estimation of the true redshift distribution of dark sirens can be obtained (refer to Zhang (2018b) for the proof). The reason is that  $E_z$  reaches maximum when the cross-correlation coefficient between surface overdensities of GW and weighted galaxies reaches maximum. This is naturally achieved when the two distributions match each other in redshift. For  $W_g$  of free functional form, the numerical variation can be challenging. However, in the context of the current paper, the situation is simpler and we can take a constrained form of  $W_g$ . Since  $m$  is the only unknown parameter,

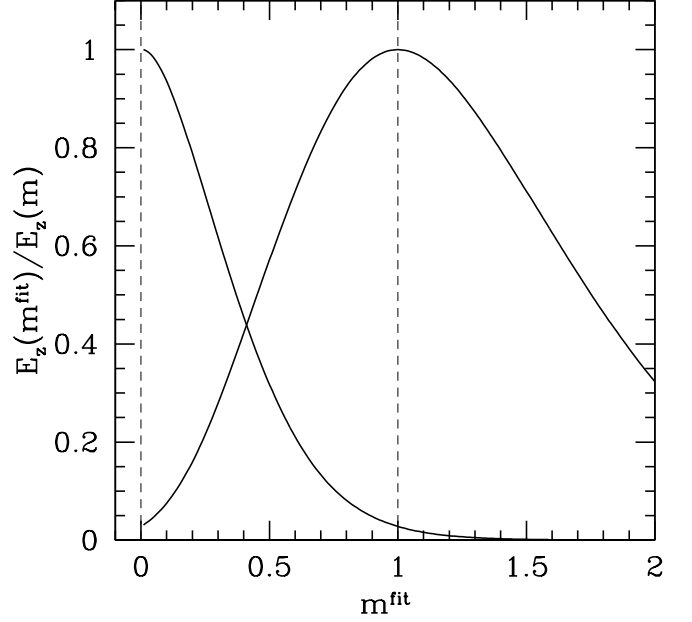


**Figure 1.**  $E_z$  as a function of the fitting parameter  $m^{\text{fit}}$ , for the luminosity bin  $D_L H_0/c \in (1.19, 1.98)$ . The fiducial  $m$  is adopted as  $m = 0$  and  $m = 1$ , respectively. Indeed,  $E_z(m^{\text{fit}})$  peaks at  $m^{\text{fit}} = m$ . Namely it provides unbiased estimation of  $m$ . We have normalized its amplitude with  $E_z(m^{\text{fit}} = m)$ .

the form of  $W_g$  can be fixed up to an unknown fitting parameter  $m^{\text{fit}}$  (namely replacing  $m$  in Eq. 2 with  $m^{\text{fit}}$ ),

$$W_g(z | m^{\text{fit}}) = \frac{\bar{n}_{\text{GW}}^{\text{cos}}(z | m^{\text{fit}})}{\bar{n}_g(z)}. \quad (9)$$

When  $m^{\text{fit}} = m^{\text{true}}$ , the weighted galaxy redshift distribution  $\bar{n}_g W_g \propto \bar{n}_{\text{GW}}^{\text{cos}}$ . Namely the weighted galaxy redshift distribution will match that of the GW redshift distribution exactly. This will result in the maximum  $E_z$ . So the form of Eq. 9 includes returns unbiased estimation of  $m$ . This is also numerically shown in Fig. 1. Therefore we will adopt this constrained form of  $W_g$ .

For brevity, hereafter we neglect the superscript “fit” in  $m^{\text{fit}}$  where it does not cause confusion with the fiducial value  $m^{\text{fid/true}}$ . The bestfit value of  $m$  is obtained when  $\partial E_z / \partial m = 0$ . Then we take the data as  $\partial E_z / \partial m$ . The posterior probability of  $m$  is

$$\begin{aligned} p(m) &\propto \exp\left(-\frac{1}{2} \Delta\chi^2\right), \\ \Delta\chi^2 &= \sum_\ell \left( \frac{\partial E_z}{\partial m} C^{-1} \frac{\partial E_z}{\partial m} \right). \end{aligned} \quad (10)$$

Here  $C$  is the covariance matrix of  $\partial E_z / \partial m$  at multipole  $\ell$ , whose full expression is given in Zhang (2018b). Statistical errors in  $\partial E_z / \partial m$  of different  $\ell$  do not correlate, so we can sum over contributions from each  $\ell$  bin to obtain the total  $\Delta\chi^2$ .

### 3 ERROR FORECAST

We apply the  $E_z$  estimator to evaluate its performance in constraining  $m$ , for third generation GW experiments such as ET and CE. We adopt the fiducial cosmology as the  $\Lambda$ CDM cosmology with  $\Omega_m = 0.268$ ,  $\Omega_\Lambda = 1 - \Omega_m$ ,  $\Omega_b = 0.044$ ,  $h = 0.71$ ,  $\sigma_8 = 0.83$  and  $n_s = 0.96$ . We consider the fiducial  $m = 1$ , as would be expected in the scenario of (Chen et al. 2019). The first question is that whether the data alone allows model-independent discrimination against the case of  $m = 0$ . If yes, then we need to verify that the bestfit indeed gives  $m = 1$  and need to quantify  $\sigma_m$ .

Implementing the  $E_z$  method requires deep and wide galaxy surveys with accurate redshift distribution. By the time of these GW experiments, stage IV spectroscopic redshifts surveys of  $\sim 10^8$  galaxies such as CSST (Zhan 2018; Gong et al. 2019), DESI (DESI Collaboration et al. 2016), Euclid (Laureijs et al. 2011), PFS (Takada et al. 2014), WFIRST (Spergel et al. 2015), and intensity mapping surveys (e.g. SKA (Santos et al. 2015) and SPHEREx (Doré et al. 2014; Dore 2018),) will likely be completed and satisfy the need. More advanced surveys with  $\sim 10^9$  galaxies with spectroscopic redshifts and deeper redshift coverage may also be available (e.g. Abdalla et al. (2015); Dodelson et al. (2016); Wang et al. (2019); Ferraro & Wilson (2019)). We also expect photometric redshift of imaging surveys such as LSST will improve to the required accuracy for implementing the  $E_z$  method. Therefore for a bin width of  $\Delta z \sim 0.2$ , we expect  $N_g$  of the order  $10^{7-8}$ .

For the GW experiments, we target at third generation experiments like ET and CE. Unlike more advanced GW experiments of percent-level accuracy in luminosity distance determination and arcminute angular resolution for both BBHs and BNSs (Cutler & Harms 2006), these experiments may only reach  $\sim 1\text{deg}^2$  in the angular resolution for BBHs (Zhao & Wen 2018). This results into a suppression of  $C_{\text{GW-g}}(\ell)$  significant at  $\ell \gtrsim 100$ ,

$$\begin{aligned} C_{\text{GW-g}}(\ell) &\rightarrow C_{\text{GW-g}}(\ell)S(\ell), \\ E_z(\ell) &\rightarrow E_z(\ell)S(\ell), \\ \frac{\partial E_z}{\partial m} &\rightarrow \frac{\partial E_z}{\partial m}S(\ell). \end{aligned} \quad (11)$$

Here  $S(\ell)$  is the suppression caused by uncertainties in the angular localization. We take a Gaussian form  $S(\ell) = \exp(-\ell^2\sigma_\theta^2/2)$ , whose effective area is  $2\pi\sigma_\theta^2$ . So the typical  $\sigma_\theta \sim 1^\circ = \pi/180$  for ET and CT.

These experiments have a typical distance error  $\sigma_D/D \lesssim 0.1$  (Zhao & Wen 2018). Therefore luminosity bin width smaller than this is unnecessary. Furthermore, the bin width needs to be sufficiently large to include enough GW events. We then choose the luminosity bins  $D_L H_0/c \in (0.51, 1.19)$ ,  $(1.19, 1.98)$ ,  $(1.98, 2.83)$ . They correspond to  $z \in (0.4, 0.8)$ ,  $(0.8, 1.2)$ ,  $(1.2, 1.6)$ , if the distance measurement is exact. The analysis can be carried out for other choices of luminosity-distance bins. The investigated ones, with bin width much larger than  $\sigma_D$ , are chosen mainly for the purpose of sufficient GW events. The number of GW dark sirens in each bin is  $\sim 10^4$ , with too large uncertainty to predict reliably. Therefore we adopt  $N_{\text{GW}} = 10^4$  as the fiducial value. Associated errors can be conveniently rescaled by  $N_{\text{GW}}^{-1/2}$  to other values. The bottom line is that we will work under the situation  $N_{\text{GW}} \sim 10^4 \ll N_g \sim 10^{7-8}$ .

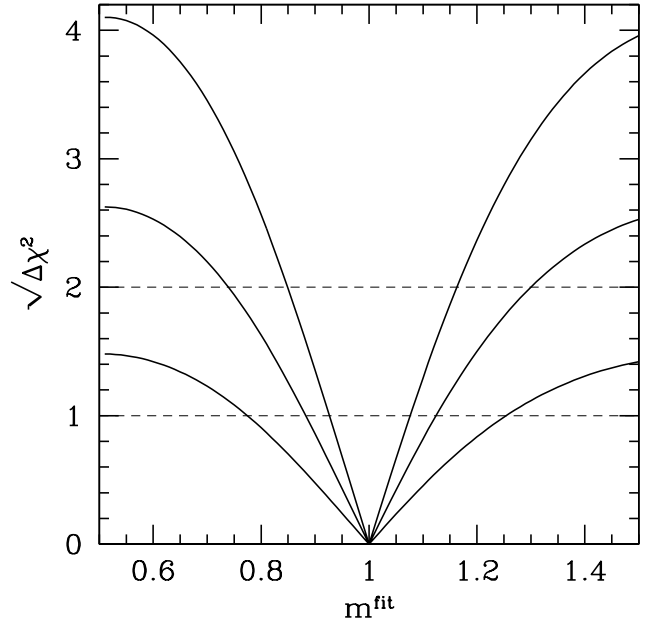


**Figure 2.**  $\sqrt{\Delta\chi^2}$  as a function of  $m^{\text{fit}}$ , which determines the posterior probability of  $m$  ( $p(m^{\text{fit}}) \propto \exp(-\Delta\chi^2/2)$ ). The fiducial  $m = 1$ . The luminosity distance range is  $(1.19, 1.98)c/H_0$ . We adopt  $N_{\text{GW}} = 10^4$ ,  $b_{\text{GW}} = 1$ ,  $\sigma_{\ln D} = 0.1$ . From top to bottom,  $\sigma_\theta = 0.5^\circ, 1^\circ, 2^\circ$  are adopted respectively. The  $1\sigma$  error in  $m$  ranges from 0.07 to 0.24.

Fig. 1 shows the dependence of  $E_z$  on the fitting parameter  $m^{\text{fit}}$ , for the luminosity bin  $D_L H_0/c \in (1.19, 1.98)$ . We show the cases of two fiducial  $m = 0.0, 1.0$  respectively. It is clear that  $E_z$  reaches the maximum when  $m^{\text{fit}} = m$ . This verifies the theoretical prediction that the  $E_z$  estimator is unbiased. Furthermore, for the same  $m^{\text{fit}}$ ,  $E_z$  of different fiducial  $m = 0, 1$  shows significant difference.

The constraining power of  $E_z$  on  $m$  is then quantified by the measurement errors in  $E_z$  and  $\partial E_z/\partial m$ . The measurement error in  $E_z$  arises both from that in  $C_{\text{GW-g}}$  and  $C_g$ . Given the availability of powerful galaxy surveys listed above, shot noise in  $C_g$  at scales of interest ( $\ell \sim 100$ ) is negligible. Namely  $C_{g,N} = 4\pi f_{\text{sky}}/N_g \ll C_g$ . But that in the GW dark siren distribution dominates over the cosmic variance. Namely the shot noise power spectrum  $C_{\text{GW,N}} = 4\pi f_{\text{sky}}/N_{\text{GW}} \gg C_{\text{GW}}$ . Therefore the statistical error  $\sigma_{E_z}$  in  $E_z$  of a multipole bin centered at  $\ell$  and with bin width  $\Delta\ell$  is dominated by error in  $C_{\text{GW-g}}$ . We then have

$$\left(\frac{E_z}{\sigma_{E_z}}\right)_\ell \simeq \frac{2\ell\Delta\ell f_{\text{sky}}}{1 + (C_{\text{GW}} + C_{\text{GW,N}})(C_g + C_{g,N})/C_{\text{GW-g}}^2}.$$

It can be further simplified,

$$\begin{aligned} \left(\frac{E_z}{\sigma_{E_z}}\right)_\ell &\simeq \frac{2\ell\Delta\ell f_{\text{sky}}}{1 + C_{\text{GW,N}}C_g/C_{\text{GW-g}}^2} \\ &\simeq \frac{2\ell\Delta\ell f_{\text{sky}}}{C_{\text{GW,N}}C_g/C_{\text{GW-g}}^2} = \frac{\ell\Delta\ell}{2\pi} N_{\text{GW}} E_z^2 \\ &\simeq 16 \left(\frac{\ell\Delta\ell}{10^4}\right) \left(\frac{N_{\text{GW}}}{10^4}\right) \left(\frac{E_z}{10^{-3}}\right)^2. \end{aligned} \quad (12)$$

**Table 1.**  $\sigma_m$ , the constraining power in  $m$ , as a function of observed luminosity distance range, angular location accuracy  $\sigma_\theta$ , and distance measurement error  $\sigma_{\ln D}$ . The fiducial multiplicative error parameter  $m = 1$ . The listed luminosity distance ranges correspond to redshift ranges (0.4, 0.8), (0.8, 1.2) and (1.2, 1.6) respectively, if we interpret them assuming  $m = 0$ .  $\sigma_\theta$  is the angular resolution, and third generation GW experiments have  $\sigma_\theta \sim 1^\circ$ . The quoted values of  $\sigma_m$  outside of the parentheses have  $\sigma_{\ln D} = 0.1$  and those inside have  $\sigma_{\ln D} = 0.2$ . The number of dark sirens within the observed luminosity-distance range is adopted as  $N_{\text{GW}} = 10^4$ .

$D_L^{\text{obs}} H_0/c$	$\sigma_\theta = 0.5^\circ$	$\sigma_\theta = 1^\circ$	$\sigma_\theta = 2^\circ$
(0.51, 1.19)	$\sigma_m = 0.07(0.11)$	0.11(0.16)	0.19(0.26)
(1.19, 1.98)	$\sigma_m = 0.07(0.12)$	0.12(0.20)	0.24(0.40)
(1.98, 2.83)	$\sigma_m = 0.08(0.15)$	0.13(0.27)	0.35(—)

Notice that  $N_{\text{GW}}$  is the total number of GW events in the sky area of the corresponding galaxy survey, which only covers a fraction  $f_{\text{sky}}$  of the whole sky.

The statistical error in  $\partial E_z/\partial m$  is  $\sigma_{\partial E_z/\partial m} = C^{1/2}$ . The full expression of  $C$  is given in Zhang (2018b). Adopting the same approximation in  $E_z$ , we have

$$\begin{aligned}
 C &\simeq \frac{1}{2\ell\Delta\ell f_{\text{sky}}} \frac{4\pi f_{\text{sky}}}{N_{\text{GW}}} \\
 &\times \frac{\int W_{g,m}^2 P_g \bar{n}_g^2 \chi^{-2} (dz/d\chi) dz}{\int W_g^2 P_g \bar{n}_g^2 \chi^{-2} (dz/d\chi) dz} \\
 &= \frac{2\pi}{\ell\Delta\ell N_{\text{GW}}} \frac{\int W_{g,m}^2 P_g \bar{n}_g^2 \chi^{-2} (dz/d\chi) dz}{\int W_g^2 P_g \bar{n}_g^2 \chi^{-2} (dz/d\chi) dz}. \quad (13)
 \end{aligned}$$

Here  $W_{g,m}(z, m) \equiv \partial W_g(z, m)/\partial m$ .

Fig. 2 shows the resulting  $\Delta\chi^2$  as a function of the fitting parameter  $m^{\text{fit}}$ , for the fiducial case of  $m = 1.0$  and the luminosity bin  $D_L H_0/c \in (1.19, 1.98)$ . We adopt  $\sigma_D/D = 0.1$  and show its dependence on the angular resolution  $\sigma_\theta$ .  $\Delta\chi^2 = 1$  determines the  $1\sigma$  error  $\sigma_m$  in the  $m$  constraint. The resulting  $\sigma_m$  is shown in Table 1. We show its dependence on the luminosity bin, angular resolution and  $\sigma_D/D$ .

In general,  $\sigma_m \sim 0.1$  is achievable. This will robustly distinguish the scenario of BBH origin with  $m = 1$  proposed in Chen et al. (2019) from the commonly assumed  $m = 0$  case. To further check these scenarios, we can split BBHs of the same luminosity bin into two samples of mass above and below  $20M_\odot$ , and apply the  $E_z$  estimator separately. If the scenario proposed by Chen et al. (2019) is valid, we will find that  $m \sim 1$  and  $\sigma_m \sim 0.1$  for the sample of  $M > 20M_\odot$ , while  $m \sim 0$  and  $\sigma_m \sim 0.1$  for the sample of  $M < 20M_\odot$ . If we apply the  $E_z$  estimator to the whole sample, we will find that  $m$  significantly deviates from zero. Furthermore, the minimum  $\Delta\chi^2$  will be significantly larger than unity, meaning bad fit of the data with a single  $m$  and multiple origins of BBHs.

There are many factors affecting the constraining power on  $m$ . Since  $C \propto N_{\text{GW}}^{-1}$  and  $dE_z/dm \propto b_{\text{GW}}$ , we have

$$\sigma_m \propto N_{\text{GW}}^{-1/2} b_{\text{GW}}^{-1}. \quad (14)$$

Here  $b_{\text{GW}}$  is the bias of GW dark sirens. We adopt  $b_{\text{GW}} = 1$  and  $N_{\text{GW}} = 10^4$  as the fiducial values. We remind that, although  $\sigma_m$  depends on  $b_{\text{GW}}$ , the bestfit  $m$  does not (Zhang 2018b). Furthermore,  $\sigma_m$  does not depend on the galaxy bias  $b_g$ , under the limit of negligible shot noise in galaxy distribution. The major limiting factor, from the observational side, is  $N_{\text{GW}}$ . Therefore the constraining power on  $m$  will also sig-

nificantly depend on the S/N threshold of GW events, which changes  $N_{\text{GW}}$  significantly.

The dependences on other factors are more complicated. These include the angular localization uncertainty  $\sigma_\theta$ , the distance measurement error  $\sigma_{\ln D}$ , the range of luminosity distance and the true value of  $m$ . One significant dependence is on  $\sigma_\theta$  (Fig. 2 & Table 1).  $\sigma_\theta$  sets the maximum  $\ell_{\text{max}} \sim 2/\sigma_\theta \simeq 115/(\sigma_\theta/1^\circ)$ , available to the given GW experiment. This factor alone would lead to  $\sigma_m \propto \sigma_\theta$ . But since shot noise also increases with increasing  $\ell$ , the dependence on  $\sigma_\theta$  is slightly weaker. The dependence of  $\sigma_m$  on  $\sigma_D/D$  is also significant, but for a different reason. Larger  $\sigma_D/D$  means wider (true) redshift distribution in GW dark sirens, making the effort of constraining  $m$  more difficult.  $\sigma_m$  increases slowly with increasing redshift/distance (Table 1), for fixed  $\sigma_\theta$ ,  $\sigma_{\ln D}$ , and  $b_{\text{GW}}$ . The reason is that same  $\ell$  means smaller  $k$  at higher redshift/distance, and therefore weaker spatial correlation signal.

## 4 DISCUSSION AND CONCLUSION

We have investigated the possibility of calibrating multiplicative errors in the dark standard siren distance determination. Such errors cause systematic deviation of the measured luminosity distance from the true cosmological luminosity distance. Through cross correlation with pre-existing galaxy redshift surveys, such systematic error can be constrained and the constraint can be made model-independent and unbiased by the proposed  $E_z$  estimator. The constraining power is mainly limited by the angular resolution and distance determination uncertainty. For ET/CE-like GW experiments,  $\sigma_m \sim 0.1$  is achievable. This constraint will provide unambiguous distinction of some BBH origin mechanisms (e.g. Chen et al. (2019)). But we caution that the discriminating power relies on the capability to appropriately select GW samples. If the selected GW sample is composed of GW events of mixed  $m$ , we may only constrain the mean  $m$ , but lose the power to identify those sub-samples with significant  $m \neq 0$ .

Multiplicate error is not the only form of systematic errors in the distance determination. Additive error with non-zero average ( $\langle \epsilon \rangle \neq 0$ ) shifts the mean value of  $D_L^{\text{obs}}$ , analogous to  $z_{\text{bias}}$  in photo- $z$  errors. Weak lensing magnification in the luminosity-distance measurement and magnification bias in the number distribution of GW events and galaxies, can also bias the inference of GW redshifts. Given the weak signal, the impact of weak lensing on  $m$  determination is negligible for  $\sigma_m \sim 0.1$ . But it may become non-negligible when  $\sigma_m$  approaches 1% or below. Other more complicated form of systematic errors may also exist. Nevertheless, the same dark siren LSS based calibration technique and the specific  $E_z$  estimator are applicable.

The expected  $\sigma_m \sim 0.1$  is for third generation GW experiments and the main limiting factors are the angular resolution and the distance determination statistical errors. Although it is already useful for certain applications, it does not meet the requirement to diagnose calibration error in GW strain measurements, or modification of GW  $D_L$  and EM  $D_L$  by modified gravity models still surviving. These applications require  $\sigma_m \sim 0.01$ . Such constraining accuracy can be achieved by more advanced surveys such as BBO.

Its arcminute resolution means that multipole modes with  $\ell \gtrsim 10^{2-3}$  are accessible. Its percent level distance determination accuracy makes a finer luminosity bin size useful. Its sensitivity to BNS events within the horizon will increase the dark siren number density by an order of magnitude, making  $\sim 10^5$  GW events per luminosity-distance bin feasible. With these threefold improvements,  $\sigma_m = 0.01$  is promising and new applications are possible.

## DATA AVAILABILITY

No new data were generated or analyzed in support of this research.

**Acknowledgement.**— This work was supported by the National Science Foundation of China 11621303 & 11653003. We thank Xian Chen for valuable information on the BBH origin mechanisms.

## REFERENCES

- Abbott B. P., et al., 2016, *Physical Review Letters*, **116**, 061102
- Abbott B. P., et al., 2017a, *Classical and Quantum Gravity*, **34**, 044001
- Abbott B. P., et al., 2017b, *Physical Review Letters*, **118**, 221101
- Abbott B. P., et al., 2017c, *Physical Review Letters*, **119**, 141101
- Abbott B. P., et al., 2017d, *Physical Review Letters*, **119**, 161101
- Abbott B. P., et al., 2017e, *Nature*, **551**, 85
- Abbott B. P., et al., 2019a, *Physical Review X*, **9**, 031040
- Abbott B. P., et al., 2019b, *ApJ*, **882**, L24
- Abbott R., et al., 2020a, arXiv e-prints, p. [arXiv:2010.14527](https://arxiv.org/abs/2010.14527)
- Abbott B. P., Abbott R., Abbott T. D., Abraham S., et al. 2020b, *ApJ*, **892**, L3
- Abbott R., Abbott T. D., Abraham S., Acernese F., et al. LIGO Scientific Collaboration Virgo Collaboration 2020c, *ApJ*, **896**, L44
- Abdalla F. B., et al., 2015, Advancing Astrophysics with the Square Kilometre Array (AASKA14), p. 17
- Ajith P., Bose S., 2009, *Phys. Rev. D*, **79**, 084032
- Arun K. G., Iyer B. R., Sathyaprakash B. S., Sinha S., van den Broeck C., 2007, *Phys. Rev. D*, **76**, 104016
- Belgacem E., Dirian Y., Foffa S., Maggiore M., 2018, *Phys. Rev. D*, **97**, 104066
- Chen X., Shen Z.-F., 2019, arXiv e-prints, p. [arXiv:1906.11055](https://arxiv.org/abs/1906.11055)
- Chen X., Li S., Cao Z., 2019, *MNRAS*, **485**, L141
- Cutler C., Harms J., 2006, *Phys. Rev. D*, **73**, 042001
- Cutler C., Holz D. E., 2009, *Phys. Rev. D*, **80**, 104009
- DESI Collaboration et al., 2016, preprint, ([arXiv:1611.00036](https://arxiv.org/abs/1611.00036))
- Deffayet C., Menou K., 2007, *ApJ*, **668**, L143
- Dodelson S., Heitmann K., Hirata C., Honscheid K., Roodman A., Seljak U., Slosar A., Trodden M., 2016, preprint, ([arXiv:1604.07626](https://arxiv.org/abs/1604.07626))
- Dore O., 2018, in 42nd COSPAR Scientific Assembly. pp E1.16–15–18
- Doré O., et al., 2014, arXiv e-prints, p. [arXiv:1412.4872](https://arxiv.org/abs/1412.4872)
- Dwyer S., Sigg D., Ballmer S. W., Barsotti L., Mavalvala N., Evans M., 2015, *Phys. Rev. D*, **91**, 082001
- Ezquiaga J. M., Zumalacárregui M., 2018, *Frontiers in Astronomy and Space Sciences*, **5**, 44
- Ferraro S., Wilson M. J., 2019, BAAS, **51**, 72
- Gong Y., et al., 2019, *ApJ*, **883**, 203
- Heymans C., et al., 2006, *MNRAS*, **368**, 1323
- Holz D. E., Hughes S. A., 2005, *ApJ*, **629**, 15
- Laureijs R., et al., 2011, preprint, ([arXiv:1110.3193](https://arxiv.org/abs/1110.3193))
- Libanore S., et al., 2020, arXiv e-prints, p. [arXiv:2007.06905](https://arxiv.org/abs/2007.06905)
- Massey R., et al., 2007, *MNRAS*, **376**, 13
- Mukherjee S., Wandelt B. D., 2018, preprint, ([arXiv:1808.06615](https://arxiv.org/abs/1808.06615))
- Nair R., Bose S., Saini T. D., 2018, *Phys. Rev. D*, **98**, 023502
- Namikawa T., 2020, arXiv e-prints, p. [arXiv:2007.04359](https://arxiv.org/abs/2007.04359)
- Namikawa T., Nishizawa A., Taruya A., 2016, *Physical Review Letters*, **116**, 121302
- Newman J. A., 2008, *ApJ*, **684**, 88
- Oguri M., 2016, *Phys. Rev. D*, **93**, 083511
- Reitze D., LIGO Laboratory: California Institute of Technology LIGO Laboratory: Massachusetts Institute of Technology LIGO Hanford Observatory LIGO Livingston Observatory 2019, BAAS, **51**, 141
- Roy S., Sengupta A. S., Arun K. G., 2019, arXiv e-prints, p. [arXiv:1910.04565](https://arxiv.org/abs/1910.04565)
- Santos M., et al., 2015, Advancing Astrophysics with the Square Kilometre Array (AASKA14), p. 19
- Schneider M., Knox L., Zhan H., Connolly A., 2006, *ApJ*, **651**, 14
- Schutz B. F., 1986, *Nature*, **323**, 310
- Shao J., Zhang P., Lin W., Jing Y., 2011, *ApJ*, **730**, 127
- Soares-Santos M., et al., 2019, *ApJ*, **876**, L7
- Spergel D., et al., 2015, preprint, ([arXiv:1503.03757](https://arxiv.org/abs/1503.03757))
- Sun L., et al., 2020, arXiv e-prints, p. [arXiv:2005.02531](https://arxiv.org/abs/2005.02531)
- Takada M., et al., 2014, *PASJ*, **66**, R1
- The LIGO Scientific Collaboration the Virgo Collaboration Abbott B. P., Abbott R., et al. 2019, arXiv e-prints, p. [arXiv:1908.06060](https://arxiv.org/abs/1908.06060)
- The LIGO Scientific Collaboration the Virgo Collaboration Abbott R., et al. 2020a, arXiv e-prints, p. [arXiv:2004.08342](https://arxiv.org/abs/2004.08342)
- The LIGO Scientific Collaboration et al., 2020b, arXiv e-prints, p. [arXiv:2010.14533](https://arxiv.org/abs/2010.14533)
- Van Den Broeck C., Sengupta A. S., 2007, *Classical and Quantum Gravity*, **24**, 1089
- Wang Y., et al., 2019, BAAS, **51**, 508
- Zhan H., 2018, in 42nd COSPAR Scientific Assembly. pp E1.16–4–18
- Zhang P., 2018a, preprint, ([arXiv:1810.11915](https://arxiv.org/abs/1810.11915))
- Zhang P., 2018b, arXiv e-prints, p. [arXiv:1811.07136](https://arxiv.org/abs/1811.07136)
- Zhang P., Pen U.-L., 2001, *ApJ*, **549**, 18
- Zhang P., Pen U.-L., Bernstein G., 2010, *MNRAS*, **405**, 359
- Zhang L., Yu Y., Zhang P., 2017, *ApJ*, **848**, 44
- Zhao W., Wen L., 2018, *Phys. Rev. D*, **97**, 064031